

Simultaneous determination of hydroquinone and catechol using a modified glassy carbon electrode by ruthenium red/carbon nanotube

Mohammad Mehdi Foroughi · Meissam Noroozifar ·
Mozhgan Khorasani-Motlagh

Received: 15 December 2013 / Accepted: 16 December 2014 / Published online: 9 January 2015
© Iranian Chemical Society 2015

Abstract A decorated glassy carbon (GC) electrode with functionalized multi-walled carbon nanotube (CNTs) and ruthenium red (RR) has been used for simultaneous determination of hydroquinone (HQ) and catechol (CC). The electrocatalytic behaviors of the GC/CNTs–RR were studied in acetate buffer solution with pH 4.5 by differential pulse voltammetry and chronoamperometry techniques. Due to the excellent electrocatalytic activity and enhanced electrical conductivity of the CNTs–RR, the simultaneous determination of HQ and CC with two well-defined peaks was achieved at the GC/CNTs–RR modified electrode. The catalytic peak currents linearly depend on the HQ and CC concentrations in the range of 1.3–433.3 μM with the sensitivity of $5.0 \mu\text{A } \mu\text{M}^{-1} \text{cm}^{-2}$ and $7.45 \mu\text{A } \mu\text{M}^{-1} \text{cm}^{-2}$, respectively. The detection limits for HQ and CC were obtained 0.21 and 0.18 μM . The diffusion coefficient for the oxidation of HQ and CC at the modified electrode was calculated as $1.06 \pm 0.05 \times 10^{-6}$ and $1.76 \pm 0.07 \times 10^{-5} \text{cm}^2 \text{s}^{-1}$, respectively. The proposed sensor was successfully examined for real water samples analysis and revealed stable and reliable recovery data.

Keywords Multi-walled carbon nanotube · Ruthenium red · Simultaneous determination · Hydroquinone · Catechol

Introduction

Phenolic compounds are ubiquitous in nature since they are formed during biological degradation processes. These compounds are used in a large number of industries, such as coal mining, oil refinery, paint, polymer and pharmaceutical preparation [1]. The two most significant isomers of phenolic compounds are hydroquinone (1, 4-dihydroxybenzene, $\text{C}_6\text{H}_6\text{O}_2$) (HQ) and catechol (1, 2-dihydroxybenzene, $\text{C}_6\text{H}_6\text{O}_2$) (CC), which are considered environmental pollutants by the US Environmental Protection Agency and the European Union [2]. Their simultaneous determination is of great necessity for environmental analysis because they coexist in environmental samples and are difficult to degrade as environmental pollutants with high toxicity [3, 4]. The CC is also found in cigarette smoke [5] and studies show that it induces damage to DNA and can cause cancer in humans [6, 7]. Therefore, it is necessary to develop simple, cheap and rapid analytical method for speciation of dihydroxybenzene isomers. So far, many methods have been established for their determination, including liquid chromatography [8, 9], synchronous fluorescence [10], chemiluminescence [11, 12], spectrophotometry [13], gas chromatography/mass spectrometry [14], pH based-flow injection analysis [15], capillary zone electrophoresis [16] and different electrochemical methods [17–24]. Electrochemical methods possess some advantages such as facile and fast operation, low maintenance costs and high sensitivity. However, a major problem is that the oxidation–reduction peak potentials of the isomers are too close at an unmodified electrode, which results in overlapping voltammetric responses making their discrimination highly difficult. A chemically modified electrode is an excellent approach to address the signal separation problem by introducing a modifier with which the extent of the interaction

M. M. Foroughi · M. Noroozifar (✉)
Analytical Research Laboratory, Department of Chemistry,
University of Sistan and Baluchestan, P.O. Box 98155-147,
Zahedan, Iran
e-mail: mnoroozifar@chem.usb.ac.ir

M. Khorasani-Motlagh
Inorganic Research Laboratory, Department of Chemistry,
University of Sistan and Baluchestan, Zahedan, Iran

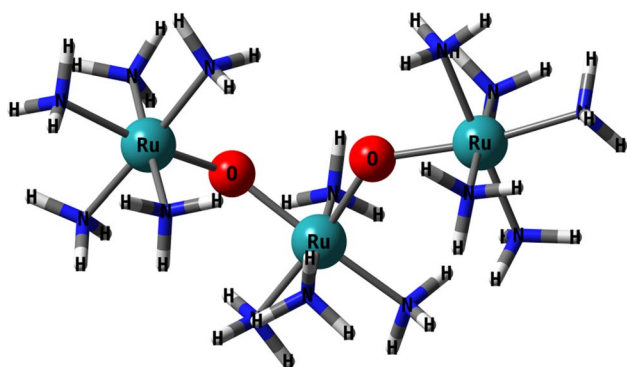


Fig. 1 The chemical structure of Ruthenium Red

differs significantly from analyte to analyte. There are some motivations behind the modification of the solid electrode surface such as improving electrocatalysis property, decreasing of surface fouling and prevention of undesirable reactions competing kinetically with the desired electrode process. Hence, various modified electrodes have been constructed for the determination of HQ and CC such as modified glassy carbon electrode (GCE) by poly(3,4-ethylenedioxythiophene)/nitrogen-doped graphene [20], poly-amidosulfonic acid-CNTs [25], ionic liquid-modified carbon paste electrode [26], poly(*p*-aminobenzoic acid [27], penicillamine) [28], Zn/Al-layered double hydroxide film [29], boron-doped diamond [30].

The carbon nanotube (CNTs), a new form of elementary carbon, is composed of graphitic sheets rolled into closed concentric cylinders with diameter of nanometers and length of micrometers [31]. Since the discovery of CNTs in 1991 [32], numerous investigations were focused on the studies of their properties and applications [33–35]. The subtle electronic properties suggest that CNTs have the ability to promote charge-transfer reactions when used as an electrode [36, 37]. It has been reported that carbon nanotubes-modified electrodes were successfully applied to study and determine many biological and organic molecules [38–42].

Ruthenium Red (ammoniated ruthenium oxychloride), (RR) is an inorganic dye (see Fig. 1) and it is used in histology to stain aldehyde-fixed mucopolysaccharides and it is used as a pharmacological tool to study specific cellular mechanisms. Selectivity is a significant issue in such studies as RR is known to interact with a large number of proteins [43]. It is a potent inhibitor of intracellular calcium release by Ryanodine receptors and displays nanomolar potency against several of its binding partners such as TRPV4, Ryanodine receptors [44].

To the best of our knowledge, no study has been reported for the electroanalysis and simultaneous determination of HQ and CC using a modified GC electrode by CNTs–RR nanocomposite. This paper includes the preparation of a

new modified GC electrode based on CNTs–RR dispersed in Nafion (NF) for the electroanalysis and simultaneous determination of HQ and CC. The voltammetric peaks of HQ and CC were well-defined at the proposed modified GC electrode. Low detection limits and high sensitivity for these two species were obtained due to the high electrocatalytic properties of RR. We evaluated analytical performance of this sensor for simultaneous determination of HQ and CC by differential pulse voltammetry (DPV). Finally, this sensor has been used for the determination of these compounds in real samples.

Experimental

Reagents and solutions

The HQ and CC were purchased from Sigma-Aldrich and used as received. A 1.0×10^{-3} mol L⁻¹ HQ and CC solution was prepared daily by dissolving appropriate amount of HQ and CC in water and the solution was diluted to 100 mL with water in a 100 mL volumetric flask. The solution was kept in a refrigerator in dark. Inorganic dye-ammoniated ruthenium oxychloride, a polycationic dye, was purchased from Merck. Nafion (5%) was purchased from Aldrich. Multi-walled carbon nanotubes with nanotube diameters, OD = 20–30 nm, wall thickness = 1–2 nm, length = 0.5–2 μm and purity of >95% was purchased from Aldrich. Dichloroacetic acid, chloroacetic acid and acetic acid were purchased from May & Bayker and Merck company. Dichloroacetic acid (pK_a = 1.26) was used for preparation of buffer solutions between pH 1.0 and 1.8, it was prepared by adjusting it to desired pH with 0.1 mol L⁻¹ NaOH solution. In a same way, chloroacetic acid (pK_a = 2.87) for pH between 1.8 and 3.8 and acetic acid (pK_a = 4.76) for pH between 3.8 and 5.6 were used.

Apparatus

Electrochemical measurements were performed with an SAMA500 Electroanalyser (SAMA Research Center, Iran) controlled by a personal computer. The three-electrode cell system consisted of GCE glassy carbon working electrode with diameter 2 mm as working electrode, a saturated calomel electrode (SCE) as reference electrode and a Pt-wire electrode as auxiliary electrode. All the electrochemical experiments were carried out under a pure nitrogen atmosphere at room temperature. TEM images were taken using a Philips CM120 transmission electron microscopy with 2.5 Å resolution.

Preparation of the modified electrode

Functionalized CNTs were first subjected to the oxidative pretreatment by vigorously stirring in a mixture of

concentrated sulfuric acid and nitric acid with the volumetric ratio of 3:1 at room temperature for 24 h. This pretreatment removes impurities and generates sufficient functional groups on the surface of CNTs [42]. The treated CNTs were filtered by centrifugation (2,000 rpm) and washed with double distilled water until the pH of the filtrate reached 7. After further washing and drying, 25 mg of CNTs was sonicated in 1.0 mL of RR solution (0.004 M) and 50 μL NF for 2 h. This mixture was denoted as CNT-RR-NF and used for electrode modification. The GC/CNTs-NF and GC/RR-NF were also prepared with the same method. The glassy carbon (GC) electrodes with 0.0314 cm^2 surface area were polished with 0.05 μm alumina slurry to a mirror finish surface and then, they were rinsed with distilled water. The GC was subsequently sonicated in a mixture of water:ethanol (9:1 v/v) for 3 min. The GCE was cleaned and activated in an electrochemical cell containing 1.0 M of deoxygenated H_2SO_4 using cyclic voltammetry between -1.5 and $+1.5$ V at a scan rate of 100 mV/s until a stable cyclic voltammetric profile (≈ 15 times) was obtained. The clean GCE was coated by casting 5.0 μL of the CNT-RR-NF or CNTs-NF suspension and then put the electrode under infrared radiation for fast drying. This modified GC electrode was denoted as GC/CNTs-RR-NF. When not in use, the modified electrode was stored in double distilled water (DDW). The GC/RR-NF and GC/CNTs-NF were also prepared with the same method.

Results and discussion

TEM characterization

Figure 2 shows the TEM images of prepared CNTs-RR-NF and CNTs-NF. In the presence of NF, the CNTs and CNTs-RR are not aggregated. The probable reason is that NF as a polymer can interact with CNTs and make heavily entangled CNTs bundles from finer bundles.

Electrochemical properties of GC/CNTs-RR-NF

Cyclic voltammograms of GC/CNTs-RR-NF in acetic acid buffer solution (AABS) (pH 4.5) at different scan rates are shown in Fig. 3a. A pair of reduction and oxidation peak at -0.193 and -0.36 V with potential peak separation $\Delta E_p = -0.17$ V was obtained. The corresponding plot for the anodic peak current (I_{pa}) and cathodic peak current (I_{pc}) as a function of scan rate (ν) (see Fig. 3b) was linearly dependent on the scan rate (ν) over the range of 25–800 mVs^{-1} , with the regression equation I_{pa} (μA) = $0.2159\nu + 14.27$ (correlation coefficient, $R^2 = 0.9919$) and I_{pc} (μA) = $-0.2341\nu - 19.93$ ($R^2 = 0.9901$), indicating a surface-controlled electrode

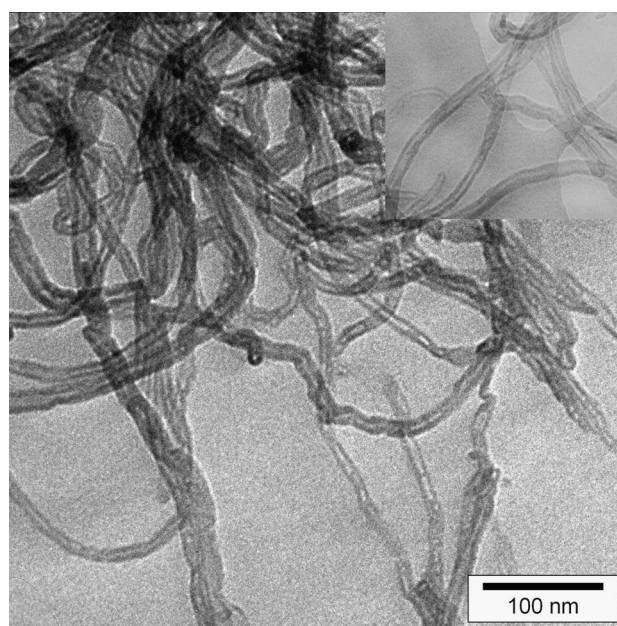


Fig. 2 TEM image of CNT-RR-NF (Inset, CNTs-NF)

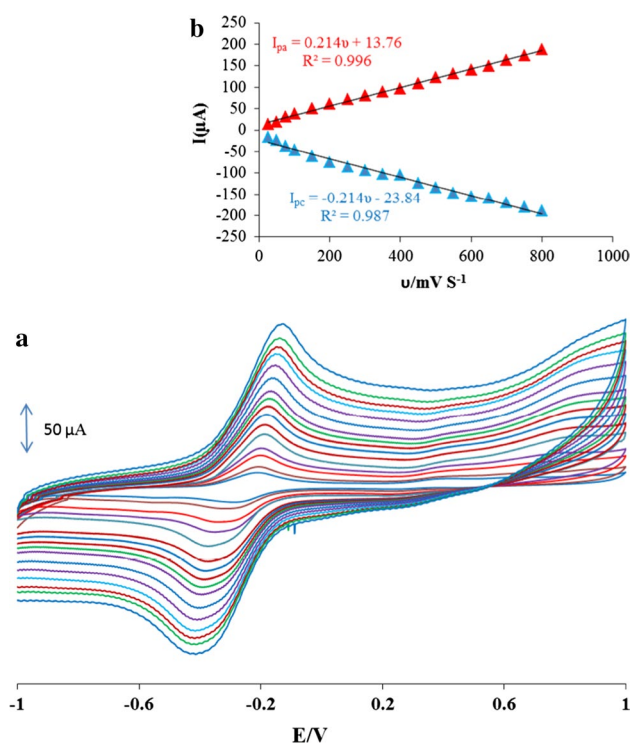
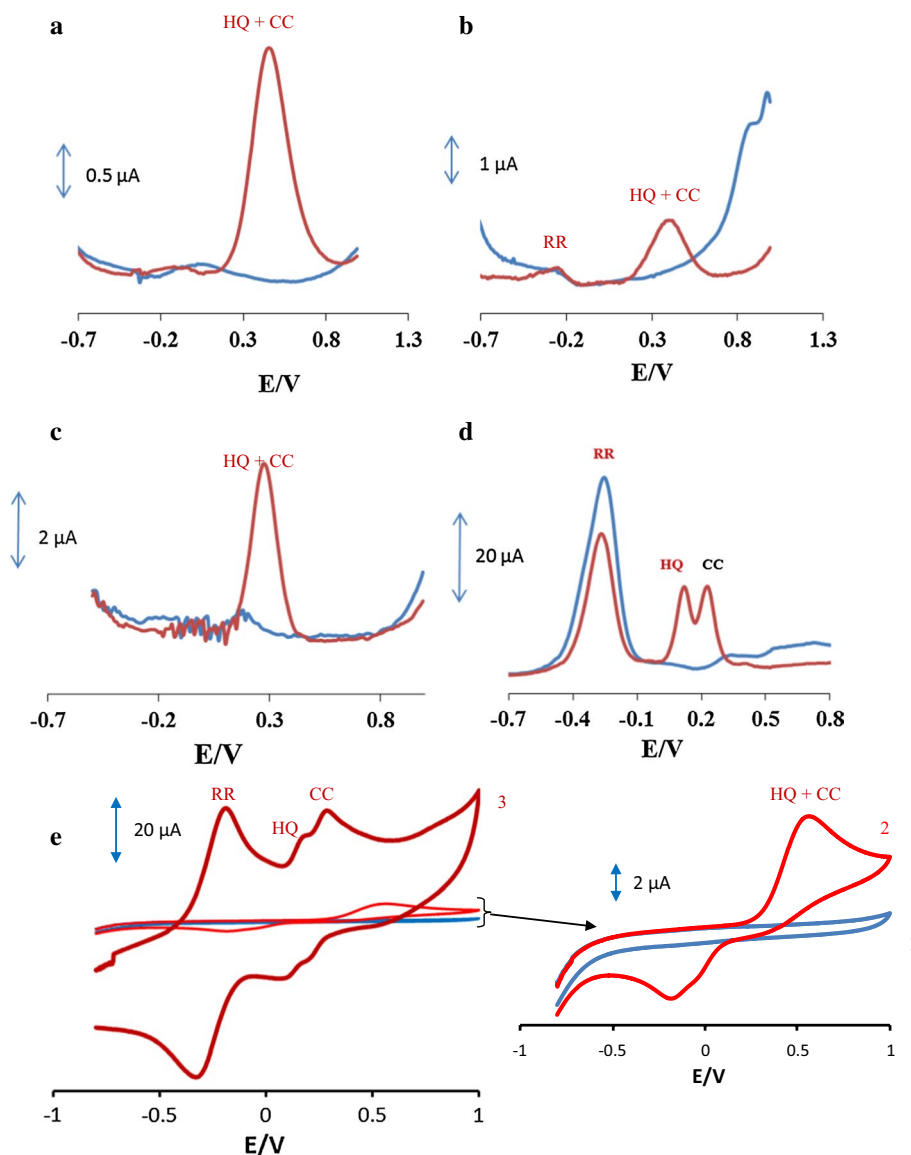


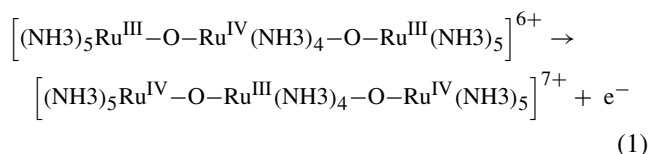
Fig. 3 a CVs of GCE/CNTs-RR-NF electrode in AABS with pH 5.5 at various scan rates (from inner to outer curve): 25, 50, 75, 100, 200, 250, 300, 350, 400, 450, 500, 600, 650, 700, 750 and 800 mV s^{-1} . b The plot of peak currents vs. scan rates

processes. From the behavior of the modified GCE with scan rate, we can conclude that the electrode reaction was a diffusionless system and a quasi-reversible electron

Fig. 4 **a** DPV at BGCE, **b** GCE/RR–NF, **c** GCE/CNTs–NF, **d** GCE/CNTs–RR–NF and **e** CVs (*I*) at GC without analyte, (2) at GC and (3) at GCE/CNTs–RR–NF electrodes in the presence of HQ and CC (133.3 μ M) in AABS (0.1 M) at pH 4.5



transfer. The peaks can be attributed to redox reaction of RR ($[\text{Ru}^{\text{III}}\text{--Ru}^{\text{IV}}\text{--Ru}^{\text{III}}]$) adsorbed in GC/CNTs–RR–NF to RR-brown ($[\text{Ru}^{\text{IV}}\text{--Ru}^{\text{III}}\text{--Ru}^{\text{IV}}]$), assumed to be a one-electron transfer [45]:



An approximate estimate of the surface coverage of the electrode was made by adopting the method used by Sharp et al. [46]. Therefore, the peak current must be related to the surface concentration of electroactive species, Γ , following Eq. (2):

$$I_p = \left(n^2 F^2 A \Gamma v \right) / 4RT \quad (2)$$

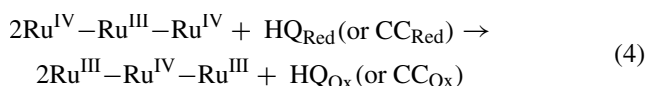
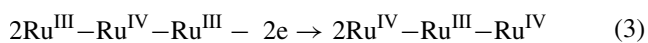
where n represents the number of electrons involved in the reaction, A is the geometric surface area of the electrode (0.0314 cm^2), Γ (mol cm^{-2}) is the surface coverage, v is the scan rate, and R , F and T have their normal meanings. From the slope 0.214 of anodic peak currents vs. scan rate (Fig. 3b), the calculated surface concentration of RR in CNTs–RR–NF is $7.15 \times 10^{-9} \text{ mol cm}^{-2}$ for $n = 1$.

Differential pulse voltammetric studies of HQ and CC

Figure 4 shows the DPVs of HQ and CC (126.6 μ M each) in 0.1 M AABS with pH 4.5 at bare GC electrode (BGC) and GC/RR–NF, GC/CNTs–NF and GC/CNTs–RR–NF-modified electrodes. BGC, GC/RR–NF and GC/CNTs–NF electrodes showed a weak oxidation peak for a mixture of HQ and CC at 0.45, 0.4 and 0.27 V, respectively (see Fig. 4a–c). Figure 4d shows the two oxidation peaks for HQ and CC at 0.118

and 0.229 V, respectively, with enhanced oxidation current response at the GC/CNTs–RR–NF electrode. Also, the peak at –0.30 V for RR redox couple was decreased. The separation of oxidation peak potential of HQ and CC was of 111 mV which was enough for the simultaneous determination of this binary mixture of HQ and CC. Based on Fig. 4b, d, oxidation peak of the RR is observed at –0.30 V on GC/RR–NF and GC/CNTs–RR–NF-modified electrodes. The oxidation peak current of RR using CNTs–RR–NF nanocomposites (Fig. 4d) was apparently higher than of RR–NF (Fig. 4b), showing the reinforcing effect of CNTs. Accordingly, CNTs–RR–NF composites can be used as promising materials for simultaneous determination of HQ and CC. The coupling of CNTs with RR has been shown to provide a cooperative and synergistic effect which can enhance the overall efficiency of the electrooxidation process. Also, Fig. 4e shows the cyclic voltammograms (CVs) in absence (see Fig. 4e₁) and a mixture of HQ and CC at unmodified GC electrode and modified GC/CNTs–RR–NF electrode. Due to comparison of proposed modified GC/CNTs–RR–NF electrode with unmodified GC electrode, GC shows just one oxidation peak for a mixture of HQ and CC at 0.52 V (see Fig. 4e₂). It is impossible to distinguish the oxidation potential of HQ and CC in the GC electrode. This revealed that the GC electrode is not suitable for the selective and stable determination of HQ and CC. Figure 4e₃ displays the CVs of a mixture of HQ and CC at GC/CNTs–RR–NF electrode. This modified electrode oxidized HQ and CC in two well-defined CV anodic peaks at 0.164 and 0.275 V and cathodic peaks at 0.073 and 0.186 V with enhanced oxidation current response for HQ and CC, respectively.

Furthermore, the oxidation peaks of HQ and CC were more stable at the GC/CNTs–RR–NF electrode in the subsequent cycles. The mechanism of this phenomenon can be written as follows:



These results showed that the electrooxidation of HQ and CC can be catalyzed by RR coupled as a mediator at the surface of the modified electrode.

The effect of pH on the oxidation of HQ and CC

The pH of the solution has a significant effect on the HQ and CC electrooxidation because protons participate in the electrode reaction [47]. The effect of pH on the oxidation of HQ and CC at GC/CNTs–RR–NF was investigated at pH levels ranging from 1.5 to 5.5 of buffer solution (0.1 mol L⁻¹) by DPVs. The results are shown in Fig. 5. Based on the results, the peak currents of HQ and CC increase

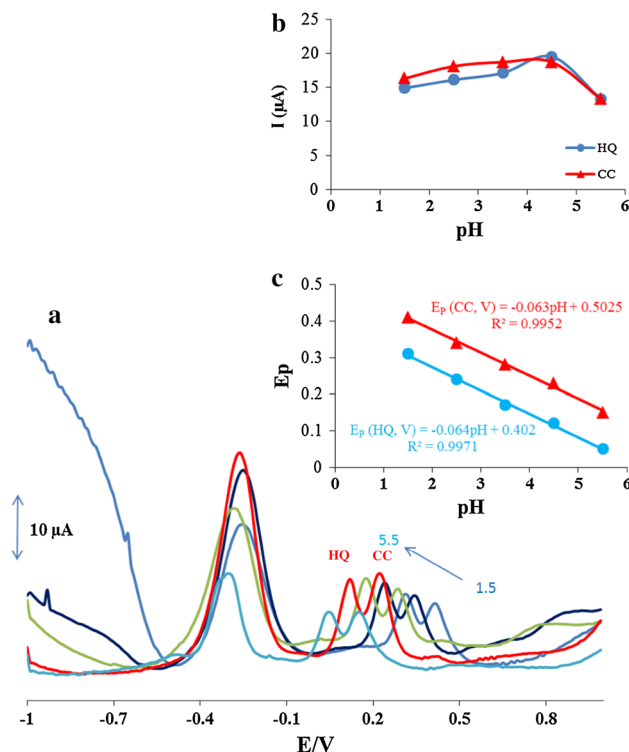


Fig. 5 a Effect of pH on the peak separation and peak current for the oxidation of HQ and CC (126.6 μM); pH = 1.5–5.5. b Plot of peak currents vs. pH and c Plot of peak potential currents vs. pH

slightly with an increase in the pH from 1.5 to 4.5 and then the peak current decreases with increase of the pH until it reaches to 5.5 (Fig. 5b). It can be seen from Fig. 5a that the highest peak current was obtained at pH 4.5 for both compounds. It was observed that as pH of the medium was gradually increased, peak potentials for the oxidation of HQ and CC shifted towards less positive values, showing that protons have taken part in their electrode processes. This was expected because of the participation of proton(s) in the oxidation reactions of HQ and CC. The oxidation reaction can be explained as follows:



where Red stands for HQ and CC; Ox stands for the responding products; *m* and *n* are the number of protons and electrons involved in the reaction, respectively. The anodic peak potentials for peak Red, is given by:

$$E'_{p(\text{Red})} = E_{p(\text{Red}, \text{pH}=0)} - \frac{2.303mRT}{nF} \text{pH} \quad (6)$$

where E_{p(Red, pH=0)} is the anodic peak potential for Red at pH = 0.0, and *R*, *T*, and *F* have their usual meanings. The value of theoretical slope, (– $\frac{2.303mRT}{nF}$), was found to be 0.059($\frac{m}{n}$) V/pH. Plot of E' _p vs. pH for HQ and CC in the working pH range is shown in Fig. 5b. As can be seen the

E'_p of both compound have linear relationship with pH of the buffer solution regarding following equations (Fig. 5b):

$$\text{HQ} : E'_p(\text{V}) = 0.402 - 0.064\text{pH} (R^2 = 0.999) \quad (7)$$

$$\text{CC} : E'_p(\text{V}) = 0.502 - 0.063\text{pH} (R^2 = 0.998) \quad (8)$$

Based on Eqs. 7 and 8, $E'_{p(\text{Red})}$ for HQ and CC were shifted to negative potentials. Regarding the observed slopes of 0.064 and 0.063 mV/pH for HQ and CC, the values were close to the anticipated Nernstian value for a two-electron, two-proton electrochemical reaction [48]. These results suggest that oxidation of HQ and CC involves an equal number of protons and electrons ($m = n$). It can be concluded that equal number of electrons and protons are involved in the electrode reactions.

Out of these, acetate buffer solution with pH 4.5 gave the best response in terms of peak current and peak shape and negative shifts, hence was chosen as optimal pH for further studies.

Interference studies

To demonstrate the selectivity of the method for the simultaneous determination of HQ and CC, the influence of potentially interfering substances on the determination of these compounds was investigated. In each experiment, the concentration of one species changed, while the concentrations of the other one were kept constant. The results are shown in Fig. 6a, b. Examination of Fig. 6a shows that the peak current of HQ increases with an increase in HQ concentration when the concentrations of CC are kept constant. Although the charge current was enhanced after HQ was oxidized, the peak currents of CC did not change. Similarly and obviously, as shown in Fig. 6b, when keeping the concentration of the HQ constant, the oxidation peak currents of CC were positively proportional to its concentration, while oxidation peak currents of HQ did not change (see Fig. 6b). The corresponding plot for the peak current as a function of concentration is shown as inset in Fig. 6c and d was linearly dependent on concentration over the range of 0.0–283.3 and 0.0–350.0 μM for HQ and CC, respectively. Also, the influence of various foreign species on the determination of 50.0 $\mu\text{mol L}^{-1}$ HQ and CC were investigated. The tolerance limit was taken as the maximum concentration of the foreign substances, which caused an approximately $\pm 5\%$ relative error in the determination of compounds. The results of this investigation are summarized in Table 1.

Simultaneous determination of HQ and CC

The DPV was performed to investigate the relationship between the peak current and concentration of two

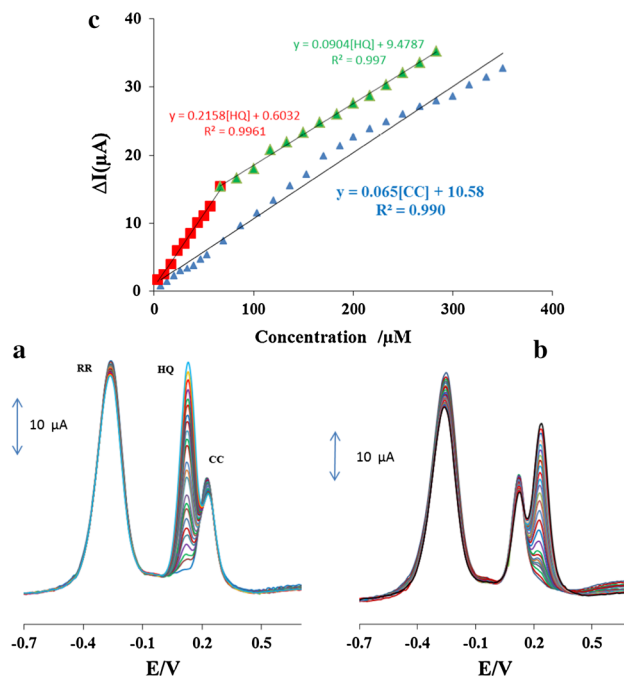


Fig. 6 DPVs at the GC/CNT-RR-NF electrode in 0.1 M pH 4.5 AABS **a** containing CC (133.3 μM and different concentrations of HQ (from inner to outer): HQ (0.0, 10.0, 16.6, 23.3, 30.0, 36.6, 43.3, 50.0, 56.6, 66.6, 83.3, 100.0, 116.6, 133.3, 150.0, 166.6, 183.3, 200.0, 216.6, 233.3, 250.0, 266.6, 283.3), **b** containing HQ (133.3 μM and different concentrations of CC (from inner to outer): CC (0.0, 6.6, 13.3, 20.0, 26.6, 33.3, 40.0, 46.6, 53.3, 70.0, 86.6, 103.3, 120.0, 136.6, 153.3, 170.0, 186.6, 200.0, 216.6, 233.3, 250.0, 266.6, 283.3, 300.0, 316.6, 33.3, 350.0) Insets: **c** Plots of I vs. concentrations of HQ and CC

Table 1 Effect of interferences on determination of 50.0 μM HQ and CC

Foreign compound	Foreign compound / HQ and CC ratio	Recovery (%)
K^+	100	97.3
Th^{4+}	100	96.0
Ca^{2+}	90	98.0
Mg^{2+}	80	99.4
Zn^{2+}	95	98
Al^{3+}	100	95.7
Cl^-	100	96.9
NO_3^-	100	101.6
SO_4^{2-}	100	97.0
Fe^{3+}	85	98.2
Resorcinol	100	99.2
Ascorbic acid	100	98.7
Urea	100	97.8

dihydroxybenzene isomers due to its higher sensitivity. As shown in Fig. 7, the DPV curves showed two well-distinguished oxidation peaks. Voltammograms clearly show

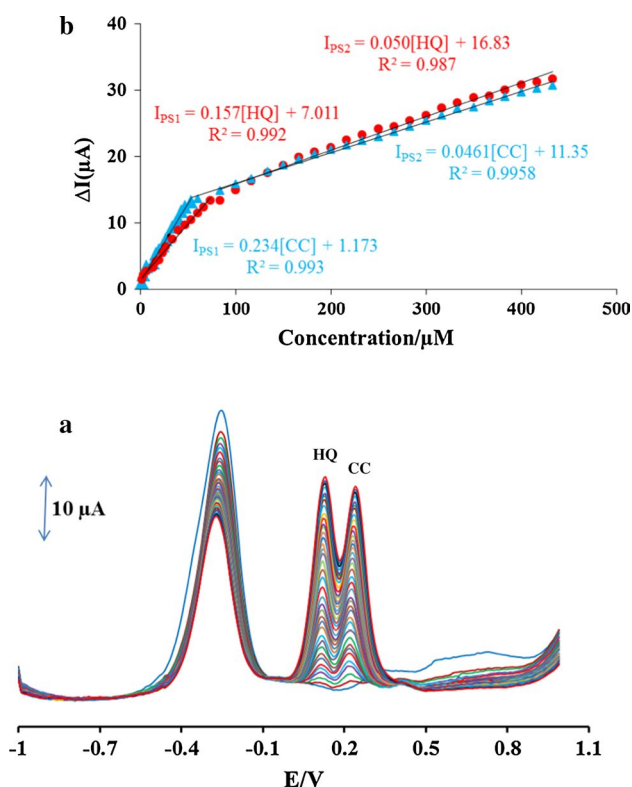


Fig. 7 a Chronoamperograms obtained at GC/CNTs–RR–NF in 0.1 M AABS (pH 4.5) for different concentration of HQ. The numbers 1–5 correspond to: 0.1, 0.3, 0.5, 1.0 and 1.5 mM of HQ. Insets b Plots of I vs. $t^{-1/2}$ obtained from chronoamperograms 1–5. c Plot of the slope of the straight lines vs. HQ concentration

that the plot of the peak current *versus* HQ and CC concentration is composed of two linear segments with different slopes (see Fig. 7c, d). The electrocatalytic peak currents for oxidation of HQ and CC at the surface of GC/CNTs–RR–NF were linearly dependent on the HQ and CC concentrations, over the range of 1.3–433.3 μ M with detection limit 0.21 and 0.18 μ M for HQ and CC, respectively. For 7 successive determinations of 66.6 μ M of HQ and CC, the relative standard deviations were 2.6 and 2.1 %, respectively. The results of the calibration characteristics at GC/CNTs–RR–NF electrode are presented in Table 2. These results show that the proposed electrode can be used

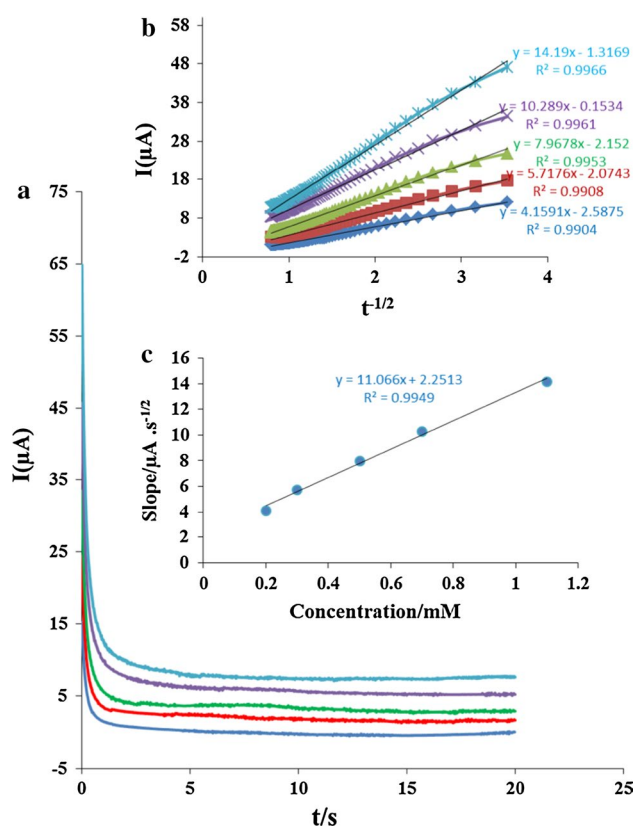


Fig. 8 a DPVs of the mixtures of, HQ and CC at the GC/CNTs–RR–NF electrode in AABS (pH 4.5). Concentrations from inner to outer of curves: HQ and CC (0.0, 1.3, 3.3, 6.6, 13.3, 20.0, 23.3, 26.6, 33.3, 40.0, 46.6, 53.3, 60.0, 66.6, 73.3, 83.3, 93.3, 100.0, 116.6, 133.3, 150.0, 166.6, 183.3, 200.0, 216.6, 233.3, 250.0, 266.6, 283.3, 300.0, 316.6, 333.3, 350.0, 366.6, 383.3, 400.0, 416.6, 433.3) Insets b Plots of I_p vs. concentration of HQ and CC

effectively for the simultaneous determination of HQ and CC.

The stability of the GC/CNTs–RR–NF electrode was studied by measuring the electrocatalytic peak currents, in repetitive potential scan cycles on different days. The electrode did not show a significant change in the peak currents of HQ and CC for more than nine months; such results could prove the stability of the modified electrode. Also, the repeatability of the modified electrode was checked for simultaneous

Table 2 Analytical characteristics of the GC/CNTs–RR–NF for determination of HQ and CC

Analyte	Linear dynamic range (μ M)		Regression equation and correlation coefficient		Detection limit (μ M)
	First segment	Second segment	First segment	Second segment	
HQ	1.3–83.3	83.3–433.3	$y = 0.157x + 7.011$ $r = 0.992$	$y = 0.05 + 16.83$ $r = 0.987$	0.21
CC	1.3–53.3	53.3–433.3	$y = 0.234x + 7.14$ $r = 0.993$	$y = 0.046x + 17.32$ $r = 0.995$	0.18

Table 3 Determination of HQ and CC in water samples using GC/CNT–RR–NF ($n = 5$)

Sample	Analyte	Detected (μM) ^a	Added (μM)	Found (μM) ^a	Recovery (%)
Tap water	HQ	ND ^b	20.0	19.4 ± 1.1	97.0
	CC	ND	50.0	48.7 ± 2.4	97.4
Well water	HQ	ND ^b	20.0	19.7	98.5
	CC	ND	50.0	49.5	99.0

^a Mean \pm standard deviation for $n = 5$

^b Not detect

determination of HQ and CC. Relative standard deviations (% RSD) for five determinations of HQ and AC (133.3 μM each) using DPV were 1.17 and 1.20 %, respectively.

Chronoamperometric study

Chronoamperometric measurements of HQ and CC at GC/CNTs–RR–NF were also studied by setting the working electrode potential at 0.25 and 0.3 V vs. SCE for the various concentration of HQ (see Fig. 8a) and CC in AABS (pH 4.5) for determination of the diffusion coefficient D . For an electroactive with a diffusion coefficient of D , the current for the electrochemical reaction with a mass transport limited rate is described by the Cottrell equation [44].

$$I = nFAD^{1/2}C_b\pi^{-1/2}t^{-1/2} \quad (9)$$

For example, under diffusion control, a plot of I vs. $t^{-1/2}$ for HQ will be linear (see Fig. 8b), and the slope of

the linear region of the Cottrell's plot can be used to estimate of the D for HQ and CC (see Fig. 8c). The value of D_{HQ} and D_{CC} were found to be $1.06 \pm 0.05 \times 10^{-6}$ and $1.75 \pm 0.07 \times 10^{-5} \text{ cm}^2 \text{ s}^{-1}$, respectively.

Real sample analysis

The modified electrode was also applied to the analysis of HQ and CC in two real samples to demonstrate the capability of the GC/CNTs–RR–NF for the simultaneous determination of HQ and CC in tap and well waters. 5 ml of each sample were added to the electrochemical cell containing 10 ml of the buffer solution and measurement was performed. The results are given in Table 3. The recoveries were found to be satisfactory (97.0 and 99.0 %) as shown in Table 3. The recovery ratio indicates that the determination of HQ and CC using the proposed electrode is effective and can be applied for the detection of HQ and CC in real samples.

Conclusions

We have demonstrated an effective electrochemical approach to construct a CNTs–RR–NF immobilized on the GCE surface and its application for the simultaneous determination of HQ and CC. Two well-defined peaks and the significant increase of peak current were observed at the GC/CNTs–RR–NF, which clearly demonstrated that RR could be used as an efficient promoter to enhance the kinetics of the electrochemical process of HQ and HQ. The

Table 4 Comparison the proposed method with other electroanalytical methods with GC/CNT–RR–NF electrodes for the simultaneous determination of HQ and CC

Modifier	Method	Linear range (μM)		Detection limit (μM)		Ref
		HQ	CC	HQ	CC	
PB-SPCE ^a	DPV	4.0–90	1.0–90	0.12	0.43	[49]
RGO–MWCNT ^b	DPV	8–391	5.5–540	2.6	1.8	[50]
ECF-CPE ^c	DPV	1–200	1–200	0.4	0.2	[51]
Au/pAMT ^d -MWCNT	DPV	7.2–391.2	3.6–183.6	0.3	0.24	[52]
Carbon nanoparticle chitosan composite	DPV	0.8–100	0.8–100	0.2	0.2	[53]
LRG ^e	DPV	1–300	2–300	0.5	0.8	[54]
PIL-MWCNT ^f	DPV	1–500	1–400	0.40	0.17	[55]
GC/CNT–RR–NF	DPV	1.3–433.3	1.3–433.3	0.21	0.18	This work

^a Prussian Blue-screen-printed carbon electrode

^b Reduced graphene oxide and multiwall carbon nanotubes hybrids

^c Electrospun carbon nanofiber-modified carbon paste electrode

^d Poly-3-amino-5-mercapto-1,2,4-triazole

^e Laser reduced graphene

^f Polymeric ionic liquid-multi-walled carbon nanotubes

optimization of the experimental conditions for differential pulse voltammetry yielded a detection limit for HQ of 0.21 μM and 0.18 for CC better than those described in the literature (Table 4).

References

- S.L. Mu, *Biosens. Bioelectron.* **21**, 1237 (2006)
- T. Xie, Q. Liu, Y. Shi, Q. Liu, *J. Chromatogr. A* **1109**, 317 (2006)
- J. Bai, L.P. Guo, J. Ndamaniha, *J. Appl. Electrochem.* **39**, 2497 (2009)
- D.D. Zhang, Y.G. Peng, H.L. Qi, *Sens. Actuator B* **136**, 113 (2009)
- I.A.R.C Working Group, *Monographs on the Evaluation of Carcinogenic Risks to Humans* p. 433 (1999)
- N. Schweigert, J.L. Acero, U. von Gunten, S. Canonica, A.J. Zehnder, R.I. Eggen, *Environ. Mol. Mutagen.* **36**, 5 (2000)
- K. Hirakawa, S. Oikawa, Y. Hiraku, I. Hirokawa, S. Kawanishi, *Chem. Res. Toxicol.* **15**, 76 (2002)
- G. Marrubini, E. Calleri, T. Coccini, A. Castoldi, L. Manzo, *Chromatographia* **62**, 25 (2005)
- A. Asan, I. Isildak, *J. Chromatogr. A* **988**, 145 (2003)
- M.F. Pistonesi, M.S.D. Nezio, M.E. Centuriñ, M.E. Palomeque, A.G. Lista, B.S.F. Band, *Talanta* **69**, 1265 (2006)
- H. Cui, Q.L. Zhang, A. Myint, X.W. Ge, L.J. Liu, *J. Photochem. Photobiol. A: Chem.* **181**, 238 (2006)
- S.F. Li, X. Li, J. Xu, X. Wei, *Talanta* **75**, 32 (2008)
- P. Nagaraja, R.A. Vasantha, K.R. Sunitha, *J. Pharm. Biomed. Anal.* **25**, 417 (2001)
- S.C. Moldoveanu, M. Kiser, *J. Chromatogr. A* **114**, 90 (2007)
- J.A. Garcia-Mesa, R. Mateos, *J. Agric. Food Chem.* **55**, 3863 (2007)
- S. Dong, L. Chi, Z. Yang, P. He, Q. Wang, Y. Fang, *J. Sep. Sci.* **32**, 3232 (2009)
- S.J. Li, Y. Xing, G.F. Wang, *Microchim. Acta* **176**, 163 (2012)
- J. Du, L. Ma, D. Shan, Y. Fan, L. Zhang, L. Wang, X. Lu, *J. Electroanal. Chem.* **722–723**, 38 (2014)
- Q. Guo, J. Huang, P. Chen, Y. Liu, H. Hou, T. You, *Sens. Actuat. B Chem.* **163**, 179 (2012)
- W. Si, W. Lei, Z. Han, Q. Hao, Y. Zhang, M. Xia, *Sens. Actuator. B Chem.* **199**, 154 (2014)
- A.T. Ezhilvillian, S.-M. Chen, L.-H. Huang, M.A. Ali, F. Al-Hemaid, *Electrochim. Acta* **125**, 503 (2014)
- M.A. Ghanem, *Electrochem. Commun.* **9**, 2501 (2007)
- H.S. Han, J.M. You, H. Seol, H. SeungwonJeon, *Sens. Actuator. B Chem.* **194**, 460–469 (2014)
- K. He, X. Wang, X. Meng, H. Zheng, S.-I. Suye, *Sens. Actuator. B Chem.* **193**, 212 (2014)
- D. Zhao, X. Zhang, L. Feng, L. Jia, S. Wang, *Colloids Surf. B* **74**, 317 (2009)
- Y. Zhang, J.B. Zheng, *Electrochim. Acta* **52**, 7210 (2007)
- P. Yang, Q. Zhu, Y. Chen, F. Wang, *J. Appl. Polym. Sci.* **113**, 2881 (2009)
- L. Wang, P. Huang, J. Bai, H. Wang, L. Zhang, Y. Zhao, *Microchim. Acta* **158**, 151 (2007)
- M. Li, F. Ni, Y. Wang, S. Xu, D. Zhang, S. Chen, L. Wang, *Electroanalysis* **21**, 1521 (2009)
- Z. Guo-Hua, T. Yi-Ting, L. Mei-Chuan, L. Yan-Zhu, *Chin. J. Chem.* **25**, 1445 (2007)
- J.N. Coleman, U. Khan, W.J. Blau, Y.K. Guñko, *Carbon* **44**, 1624 (2006)
- S. Iijima, *Nature* **354**, 56 (1991)
- F. Berti, L. Lozzi, I. Palchetti, S. Santucci, G. Marrazza, *Electrochim. Acta* **54**, 5035 (2009)
- M. Ghalkhani, S. Shahrokhian, F. Ghorbani-Bidkorbeh, *Talanta* **80**, 31 (2009)
- Q. Shen, X.i. Wang, *J. Electroanal. Chem.* **632**, 149 (2009)
- J.M. Nugent, K.S.V. Santhanam, A. Rubio, P.M. Ajayan, *Nano Lett.* **1**, 87 (2001)
- K. Gong, Y. Yan, M. Zhang, L. Su, S. Xiong, L. Mao, *Anal. Sci.* **21**, 1383 (2005)
- Y. Wang, W.Z. Wei, X.Y. Liu, X.D. Zeng, *Mater. Sci. Eng., C* **29**, 50 (2009)
- H.T. Zhao, H.X. Ju, *Anal. Biochem.* **350**, 138 (2006)
- A. Merkoci, M. Pumera, X. Llopis, B. Perez, M. del Valle, S. Alegret, *Anal. Chem.* **24**, 826 (2005)
- V.G. Gavalas, S.A. Law, J.C. Ball, R. Andrews, L.G. Bachas, *Anal. Biochem.* **329**, 247 (2004)
- Y. Lin, X. Cui, X. Ye, *Electrochem. Commun.* **7**, 267 (2005)
- F. Vincent, M.A. Duncton, *Curr. Top. Med. Chem.* **11**, 2216 (2011)
- L.X.A. Tripathy, D.A. Pasek, G. Meissner, *Ann. N. Y. Acad. Sci.* **853**, 130 (1998)
- M. Yagi, S. Tokita, K. Nagoshi, I. Ogino, M. Kaneko, *J. Chem. Soc., Faraday Trans.* **92**, 2457 (1996)
- M. Sharp, M. Petersson, K. Edström, *J. Electroanal. Chem.* **95**, 123 (1979)
- K. Nakano, K. Ohkubo, H. Taira, M. Takagi, N. Soh, T. Imato, *J. Electroanal. Chem.* **623**, 49 (2008)
- A.J. Bard, L.R. Faulkner, *Electrochemical Methods: Fundamentals and Applications*, 2nd edn. (Wiley, New York, 2001)
- M. Buleandra, A.A. Rabinca, C. Mihailciuc, A. Balan, C. Nichita, I. Stamatina, A. Al. Ciucu **203**, 824 (2014)
- F. Hu, S. Chen, C. Wang, R. Yuan, D. Yuan, *Anal. Chim. Acta* **724**, 40 (2012)
- Q. Guo, J. Huang, P. Chen, Y. Liu, H. Hou, T. You, *Sens. Actuator. B Chem.* **163**, 179 (2012)
- C. Wang, R. Yuan, Y. Chai, F. Hu, *Anal. Meth.* **4**, 1626 (2012)
- M. Amiri, S. Ghaffari, A. Bezaatpour, F. Marken, *Sens. Actuator. B Chem.* **162**, 194 (2012)
- T. Lai, W. Cai, W. Dai, J. Ye, *Electrochim. Acta* **138**, 48 (2014)
- X. Feng, W. Gao, S. Zhou, H. Shi, H. Huang, W. Song, *Anal. Chim. Acta* **805**, 36 (2013)